Scanning Microscopy

Volume 2 | Number 2 Article 23

1-25-1988

Quench Cooled Ice Crystal Imprint Size: A Micro-Method for Study of Macromolecular Hydration

Ivan L. Cameron
The University of Texas Health Science Center at San Antonio

Keithley E. Hunter
The University of Texas Health Science Center at San Antonio

Gary D. Fullerton
The University of Texas Health Science Center at San Antonio

Scanning Microscopy, Vol. 2, No. 2, 1988 (Pages 885-898) 0891-7035/88$3.00+.00
Scanning Microscopy International, Chicago (AMF O'Hare), IL 60666 USA

QUENCH COOLED ICE CRYSTAL IMPRINT SIZE: A MICRO-METHOD FOR STUDY OF MACROMOLECULAR HYDRATION

Ivan L. Cameron*, Keithley E. Hunter, and Gary D. Fullerton

Cellular and Structural Biology Department (I.L.C. and K.E.H.)
Radiology Department (G.D.F.)
The University of Texas Health Science Center
at San Antonio
San Antonio, Texas 78284

(Received for publication April 25, 1987, and in revised form January 25, 1988)

Abstract

Quench cooling (rate > 4000°C/sec) of biological specimens limits growth of ice crystals by processes different from slow cooling methods. Quench cooling in liquid propane cooled in liquid nitrogen induced ice crystal segregation compartments, as imaged by scanning transmission electron micrographs of freeze-dried cryosections of tissues and protein solutions. The observed imprints of ice crystals were relatively small and roughly spherical. The size of these ice crystal imprints increased with distance from the specimen/quenchant surface. Beyond a depth of 150 microns the size of the imprints was constant but differed among subcellular compartments. The size of the imprints was found to be dependent on: water content, extent of hydration water and the degree of protein aggregation. Determination of extent of hydration water and degree of protein aggregation in protein solutions by measurements on the size of ice crystal imprints yields data in agreement with macroscopic methods. Thus ice crystal imprints give information about the interactions of macromolecules and water at a subcellular level of resolution.

Key Words: Ice crystal imprints, cryofixation, protein hydration, protein aggregation, unfreezable water in aqueous solutions, quench cooled samples.

*Address for Correspondence:
I.L. Cameron Department of Cellular and Structural Biology The University of Texas Health Science Center at San Antonio Texas 78284, U.S.A. Phone No. (512) 567-3817

Introduction

The introduction of cryofixation of biological specimens combined with appropriate preparative procedures for electron microscopic observation have allowed the revelation of much new information about the ultrastructural organization of biological specimens especially by use of the freeze-fracture deep-etch techniques (Heuser 1981, Hirokawa, 1986). An objective in the preparation of specimens for such studies has been to get the smallest ice crystal dimensions possible so as not to disturb ultrastructural detail. Considerable effort has therefore been devoted to increasing the cooling rate with the aim of achieving a vitreous frozen state. The results have led to specimen preparations with no visible imprints of ice crystals within a few microns of the quenchant surface and in this regard the objective has been attained. As we began to visualize the size of imprints of ice crystals in thin freeze-dried cryosections of quench frozen specimens, it became clear not only that the average size of ice crystal imprints varied with the distance from the specimen/quenchant surface (fig. 1) but also within different morphological compartments of the specimen (Cameron et al.,

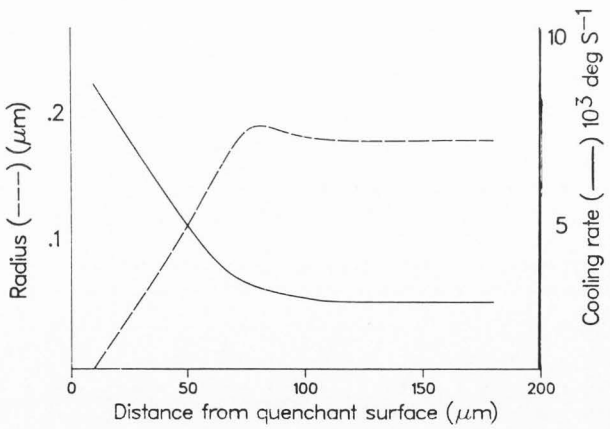

Fig. 1. Ice crystal imprint size and cooling rate in a tissue specimen as a function of distance from the quenchant surface. Modified from Cameron et al. (1985).

1985). We therefore began to ask just what this difference in size of imprints of ice crystals among tissue compartments was due to and also to ask if ice crystal imprint size could give us useful information about the interactions of macromolecules and water at a subcellular level of resolution.

Such imprints of ice crystals are created by the segregation of solutes and water during the cooling process. Freeze-drying of the frozen cryosections of the specimens removes the ice but not the solutes that encased the ice crystal. What remains is an imprint of the ice crystal which is visualized in freeze-dried cryosections. The radius of these imprints in the specimens we studied was small (< 0.5 μm) in comparison to the size of hexagonal ice crystals (> 1.0μm). Without knowledge of the crystallographic structure of the ice in our specimens we have not been able to distinguish if our imprints reflect individual cubic ice crystals or if they reflect cross sections through dendritic processes of hexagonal ice crystals. In either case the size of these imprints is determined by such factors as: the diffusion of water to the advancing ice surface, the segregation of water and solutes at least over the dimensions of the resulting ice crystal imprints, temperature gradients, and non-uniform concentration gradients, heat dissipation, and pressure gradients. A comprehensive modeling of such a complex process for biological tissues will be difficult. Nevertheless we began a series of experimental studies aimed at what the size of ice crystal imprints could tell us about the interactions of macromolecules and water (Cameron et al., 1985). The present paper reviews our past work and presents new experimental findings in support of a model to explain the observations.

Background Information for Interpretation of Quench Cooled Ice Crystal Imprint Size.

The model developed to explain the quench cooled ice crystal size data is based on a three-fraction fast-exchange model of macromolecular hydration. NMR titration studies (measurement and analysis of the proton relaxation rate at multiple levels of hydration of a specimen) on lysozyme and on bovine serum albumin have shown that the proton spin lattice (T_1) relaxation rate can be expressed by fast exchange between three main water compartments termed: bound, structured and bulk water (Fullerton et al., 1986, 1987). As there are no universally accepted terms describing hydration of proteins or of biological specimens we define and use the following terms: 1) Bulk water - water molecules so distant from solute surfaces that their molecular motion is determined only by the interaction characteristics of the water molecules themselves. 2) Hydration water - all water molecules for which motion is perturbed from that of bulk water (as defined below, hydration water is the sum of both bound and structured water). 3) Bound water - water molecules which are bound by 2 or 3 hydrogen bonds to fixed polar sites and those bound to ionic sites on the protein. 4) Structured water - water molecules that are less motionally perturbed than bound or superbound water but are still perturbed in structure from that of bulk water.

A model of protein solutions with three water compartments (bulk, structured and bound) is both necessary and sufficient to explain all the varied hydration measures made on lysozyme. These measures include: NMR titration, x-ray diffraction on protein crystals, hydration by sedimentation, isopiestic isotherms, differential scanning calorimetry, the non-freezing fraction and dielectric attenuation.

For both the protein solutions and for the tissues subjected to our quench cooling procedure, it is reasonable to assume that the size of ice crystal imprints was limited by the number of water molecules that could diffuse to an ice crystal nucleation site prior to cooling to the point where diffusion of uncrystallized water molecules was interrupted, a nonequilibrium condition. Considering that some of the water molecules on the surface of proteins are irrotationally bound (correlation times of 10^{-9} sec or less), then the diffusion of the remainder of the surface water molecules would consist of that compartment of water molecules we defined as structured water (correlation time of 10^{-11} sec), as illustrated in fig. 2.

A slower cooling rate (as in the case of contact with liquid nitrogen vapor) leads to a reproducible pseudo-equilibrium state where a fraction of unfreezable or irrotationally bound water occurs (Franks 1982). This fraction of unfreezable or bound water has, in the past, been regarded by most workers in the field as the water of hydration of the protein. Although the unfreezable water remaining after such slow cooling is in reasonable agreement with estimates of bound water obtained from several different and well accepted methods for determination of the extent of bound water (Kuntz and Kauzmann, 1974); this amount of unfreezable water does not include structured water and therefore can greatly underestimate the true extent of hydration water as reported for cells and proteins (Merta et al., 1986, Fullerton et al., 1983, 1986). The most likely reason for the past underestimates of protein hydration water is that the methods were either not designed to measure or are not sensitive enough to measure the modest differences in the motional properties of structured as compared to bulk water.

Two factors are offered to explain the observed larger ice crystal imprints in quench cooled tissues enriched in filamentous proteins (Cameron et al., 1985) or in the quench cooled specimens where aggregation of globular proteins has been demonstrated to occur (fig. 2). The first factor is that the aggregation of globular proteins displaces a portion of the hydration water which increases the bulk water fraction and that solutions or tissues enriched in long filamentous proteins have already undergone extensive polymerization of subunits into long

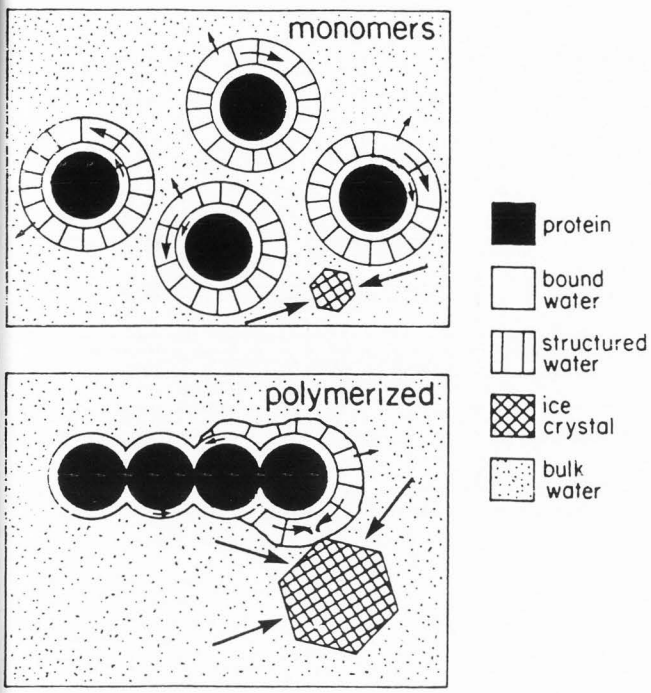

Fig. 2. Model of the effect of macromolecular aggregation on quench cooled ice crystal imprint size. The distance a water molecule can migrate in a fixed time is indicated by the length of arrows. Aggregation "frees" some of the bound and structured water yielding proportionally more bulk water and increases the length of surface that allows more structured water to migrate to a growing ice crystal prior to vitrification. Both of these factors allow larger ice crystal growth during quench cooling.

filaments. The latter therefore have less hydration water per unit dry mass of protein. The greater abundance of bulk water per unit dry mass therefore provide a proportionally larger mass of more bulk water for incorporation into a growing ice crystal during quench cooling. The second factor offered to explain the larger size of ice crystal imprints involves the possibility of faster diffusion of structured water along macromolecular surfaces. This would allow recruitment of both bulk and structured water to an ice crystal nucleation site during quench cooling.

We have previously shown that all of the water in tendon is anisotropically oriented along the long axis of the tendon filaments (Fullerton et al., 1985). We and others have also observed the anisotropy of water orientated in the long axis of the skeletal muscle fibers and aligned keratin fibrils. It has also been shown that the diffusion coefficient of water in the parallel orientation of filamentous specimens (i.e. skeletal muscle and keratin) is significantly higher than it is in the perpendicular orientation of the filamentous specimens (Hazlewood, 1979 and Lynch, 1983). Therefore it is proposed that faster diffusion of chains of longitudinally oriented (structured) water along the surface of filamentous proteins is rapid enough to allow water molecules to migrate further prior to the point where diffusion of uncrystallized water molecules is interrupted (a nonequilibrium condition). The ice crystal is larger because more water molecules can arrive during the time before diffusion of uncrystallized water is interrupted by quench cooling.

Materials and Methods

Human hemoglobin (Sigma Chem. Co., St. Louis, Mo., Cat. No. H7379, 2X crystallized, dialyzed and lyophilized) was used with no further purification. Lysozyme (Sigma Chem. Co. grade 1) three times recrystallized, dialyzed and lyophilized was used with no further purification. Bovine serum albumin, fraction V (Sigma Chem. Co., Cat. No. A-4503), was used with no further purification. Actin was also purchased from Sigma Chem. Co. or was prepared from chicken muscle using a modification of the procedure of Spudick and Watts (1971). The lyophilized powdered actin was greater than 90% G-actin, as shown by SDS polyacrylamide gel electrophoresis and contained approximately 5% Tris as supplied. A 12.4 mg/ml solution was made by dissolving the actin in deionized water. The actin was polymerized by adding potassium chloride to a desired concentration (Bryan and Kane, 1982). Gelation was observed macroscopically as an increase in viscosity, and polymerization (aggregation) was noted microscopically by the presence of protein mats, as well as by the observation in the scanning transmission electron microscope of protein crystals (an indication of further aggregation) in quench cooled freeze dried cryosections.

Samples of tissue from decapitated adult male rats as well as the lens and Achilles' tendon from freshly slaughtered cows were used for the ice crystal imprint size measurements, for water content measurements, and for scanning transmission electron microscopy. Fully grown oocytes were also removed from adult Xenopus laevis ovaries (LaBadie et al., 1981) for ice crystal imprint size studies. Water content of all specimens was determined by difference in wet and dry weight using procedures previously described (Cameron et al., 1983).

The methods for quench cooling of specimens and for processing of specimens for size of ice crystal imprint measurements have been described previously but are repeated here for completeness. The specimens (1-2 mm^3) were placed on a brass stub, and were quench cooled by rapid immersion in liquid propane cooled in a liquid nitrogen bath (see Elder et al., 1982 for details of cooling conditions). This procedure is reported to give rapid cooling rates (4,000 to 5,000°C/sec at the surface of the specimen) which compare well to the cooling rates of tissue slammed onto copper and mercury surfaces (Elder et al., 1982; Rebhun, 1972; and Schwabe and Terracio, 1980). The specimen was then prepared by one of two procedures.

In one procedure, the rapidly cryofixed specimens were transferred to a cryostat (Harris Mfg. Co., N. Billerica, MS) maintained at -30°C. After two hours of temperature equilibration 2 μm-thick sections were cut with a Minot custom microtome (Damon/IEC Div., Damon Corp, Needham Heights, MA). Within the -30°C cryostat chamber, the 2 μm-thick sections were positioned on a film of Formvar (0.9% in dioxane) spanning a 1.5 mm hole in a 3 mm carbon grid. To minimize curling or movement of the sections, a cover, precooled to -30°C, was laid over the sections. The cover consisted of a circular piece of heavy aluminum with a carbon coated Formvar film stretched across a hole in the center. Thus, the section was placed or "sandwiched" between two films of Formvar. The sandwiched specimen was cryoadsorbed for 16 h at -30°C in a custom made cryoabsorption apparatus, warmed to room temperature, vented with nitrogen gas and stored in a desiccator. At the time of analysis the aluminum ring was teased away, leaving a flat dried section sandwiched between two layers of Formvar film. The sandwiched sections were examined at 25kV in a JEOL-35 scanning electron microscope. Morphology of the specimens was recorded by photographing the transmitted image from the recording cathode ray tube at 5000X.

In the other procedure, cryofixed samples were allowed to warm to -100°C and thin sectioned (0.1 μm) on an LKB Ultratome V equipped with a modified cryokit which was kept cooled to a temperature of -100°C for both specimen and knife (Cameron et al., 1983). A dry glass knife with a 40° angle and a sectioning speed of 10 mm/s was used for cutting. Sections were obtained by advancing 0.1-1μm on the microfeed. The sandwiched specimen was dried within the LKB chamber at -100°C in a custom-made cryosorption apparatus by evacuation with a rotary pump for 2 h. The sections were then allowed to warm to room temperature in the vacuum apparatus, vented with dry nitrogen gas, and stored in a desiccator. In some cases blocks of uncut specimens which had been cryosectioned at -100°C in the LKB cryostat were transferred to the Harris cryostat allowed to warm to -30°C and more cryosections were made and processed as described above.

To measure size of ice crystal imprints, the photographic negatives of the cryosectioned specimens were enlarged to a constant size, and the edges of the projected and contiguous ice imprints were traced with a pencil on paper. All ice crystal imprints in a localized area were traced to assure that a representative sampling was taken. In cases where shades of grey existed between the center and the edge of the ice crystal imprint, the outer limit of the recognizable imprint was traced. A standard EM replicate grading scale was photographed under the same conditions as the tissues, and served as a dimension reference. The area of tracings of ice crystal imprint were then measured with a planimeter. After corrections for magnification, the maximal cross sectional area of the ice crystal imprint size was calculated in m^2. In many cases the radius (r) of ice crystal imprints was calculated based on their mean cross sectional area and assuming spherical shape. The formula used for conversion, of cross sectional area (A) to the radius was $r = \sqrt{A/\pi}$.

A least squares linear regression was performed on the data. The statistical analyses were done in a computer resource center using The Statistical Package for Social Sciences SPSS).

Results and Discussion

Standardization and Validation of the Quench Cooled Ice Crystal Imprint Size Method.

The rate of cooling as well as the concentration and nature of the solute influence the ice crystal imprint growth rate and shape in aqueous solutions (Franks, 1982). As the cooling rate of a specimen is fastest at the surface in contact with the quenchant one expects the ice crystal imprint size of an aqueous solution of a globular protein to increase as a function of distance from the quenchant surface. Figure 3 illustrates that this is indeed true in the case of a freeze-dried cryosection of a quench cooled drop (1-2 mm^3) of a 16% w/w solution of bovine serum albumin (BSA). Such an increase in ice crystal imprint size in rapidly cooled specimens has been reported by several other workers (Andrews et al., 1983; Elder et al., 1982; Frederick and Busing, 1981; Rapatz et al., 1966; and van Venrooij et al., 1975). A plot of the size of ice crystal imprints within BSA solution as well as in other biological soft tissue specimens has shown that a plateau in size was reached by 150 μm distance within the specimens (Cameron et al., 1985). A uniform mean ice crystal imprint size deeper within rapidly cooled biological specimens has also been reported by Elder, et al., (1982).

The finding of uniform mean ice crystal imprint size at distances of 150 μm or greater from the quenchant surface indicated that our method of cooling might be a reproducible and a reliable procedure for determination and comparison of ice crystal imprint size both between specimens and among subcellular compartments within a specimen. Several observations support this idea as reviewed next.

Because some of our cryosections were cut at -100°C, while others were cut at -30°C, we questioned if the size of ice crystal imprints would depend on the cutting temperature. Although it seemed possible that significant ice recrystallization might have occurred upon warming the specimens to -30°C, several types of observations suggest that the ice crystal imprint size, generated at the time of quench cooling in liquid propane, was maintained upon warming to -30°C. The first observation to support this claim is that no ice crystal imprints appeared at the specimen surface in the zone where no ice crystal imprints originally formed; in our experiment the hydrated cryosection was warmed from -100°C to -30°C

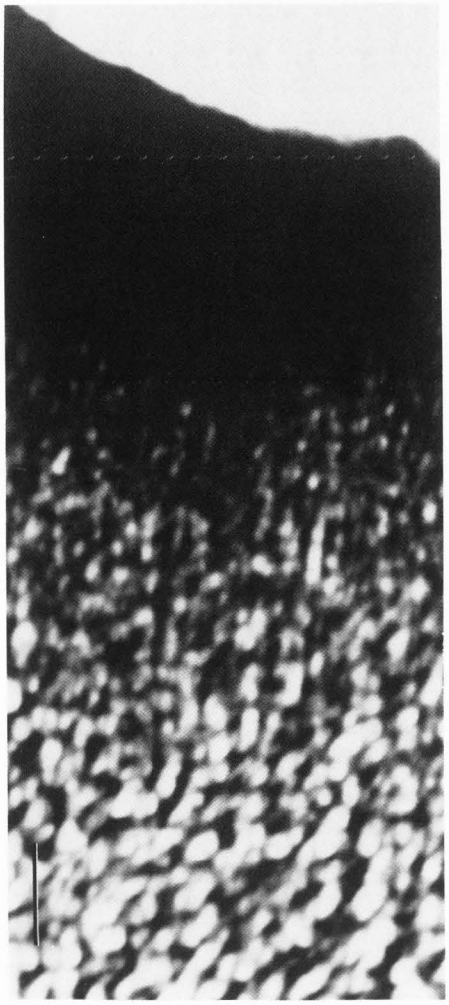

Fig. 3. Electron micrograph of a 2 μm thick freeze-dried cryosection of bovine albumin (BSA) solution of 84% water content. An increase in the size of ice crystal imprints at various depths from the BSA/quenchant interface is shown. The tissue was quenched in liquid propane at -169°C; the cryosectioning and cryoadsorption were done at -30°C. Bar = 1.0 μm.

prior to cryoadsorption. Another procedure used to validate this interpretation, was to cut and process cryosections at -100°C as compared with cutting and processing of cryosections from the same specimen at -30°C. At a distance of greater than 150 μm from the specimen surface the mean size of ice crystal imprints was not significantly different for the two different handling temperatures (Cameron, et al., 1985). Because the cryosections maintained the same ice crystal imprint vs. depth profile from the specimen surface at the two different temperatures we conclude that the history of ice crystal formation is accurately reflected in the imprints in the cryosections, even when cut at -30°C. This conclusion does not imply that significant translocation of ions has not occurred at the higher temperature for it has been shown that some ions can translocate at a cellular level of resolution at -30°C (Cameron et al., 1983). We do, however, claim that raising the temperature to -30°C did not change the size of the ice crystal imprints generated at the time of cryofixation.

When similar specimens were cooled more slowly, i.e., in liquid nitrogen vapor, ice crystal imprints of larger size were observed at the surface and throughout the specimen. This finding serves as a control to show that larger sized ice crystal imprints are formed if the cooling rate is slower and that ice crystals can grow even at the specimen surface.

Another argument in favor of the idea that the ice crystal imprints seen at 150 μm or more depths within the quench cooled specimens reveal the true history of the cooling event is based on data from MacKenzie (1981) and from Franks (1982). Because quench cooling leads to incomplete crystallization, the interrupted freezing process will continue at some temperature during warming of the specimen. This process is called recrystallization. One may expect growth in the mean ice crystal imprint size at the point of recrystallization. MacKenzie (1981) reported that thermal instabilities in slowly warmed gelatin gels that had been rapidly cooled, occurred when the gels were at remarkably high temperatures. For example, rapidly cooled gelatin gels with a 28.6% and a 40.0% wt/wt gelatin concentration showed antemelting at -23.1°C and -21.2°C, respectively. These gels showed well defined exotherms (indicating migratory recrystallization and grain growth) at -6.3 and -9.8°C, respectively. Likewise Franks (1982) summarizes the recrystallization temperatures of four rapidly-quenched aqueous protein solutions. The recrystallization temperatures were reported to be: gelatin -11°C, ovalbumin -10°C, bovine serum albumin -5.3°C and hemoglobin -3.5°C. Thus, all available evidence indicates that it is only necessary to keep a rapidly cooled specimen below its antemelting temperature to prevent recrystallization of the ice crystals. This supports the idea that the ice crystal imprints observed after the liquid propane quench and our handling procedures give a true measure of the history of ice crystal growth at the time of the initial quench.

Based on the above we conclude that our method of cryofixation, cryosectioning and freeze-drying yields a reproducible method for the study of ice crystal imprints that were generated at the time of quench cooling in the biological specimens.

Differences in Ice Crystal Imprint Size Among Tissues and Subcellular Compartments.

The micrographs in plate 1 (figures 4-10) illustrate many of our scanning transmission electron microscopic observations on freeze-dried cryosections of cells and tissues that were rapidly cooled in liquid propane cooled in a liquid nitrogen bath. All of the micrographs in plate 1 are of the same magnification so that

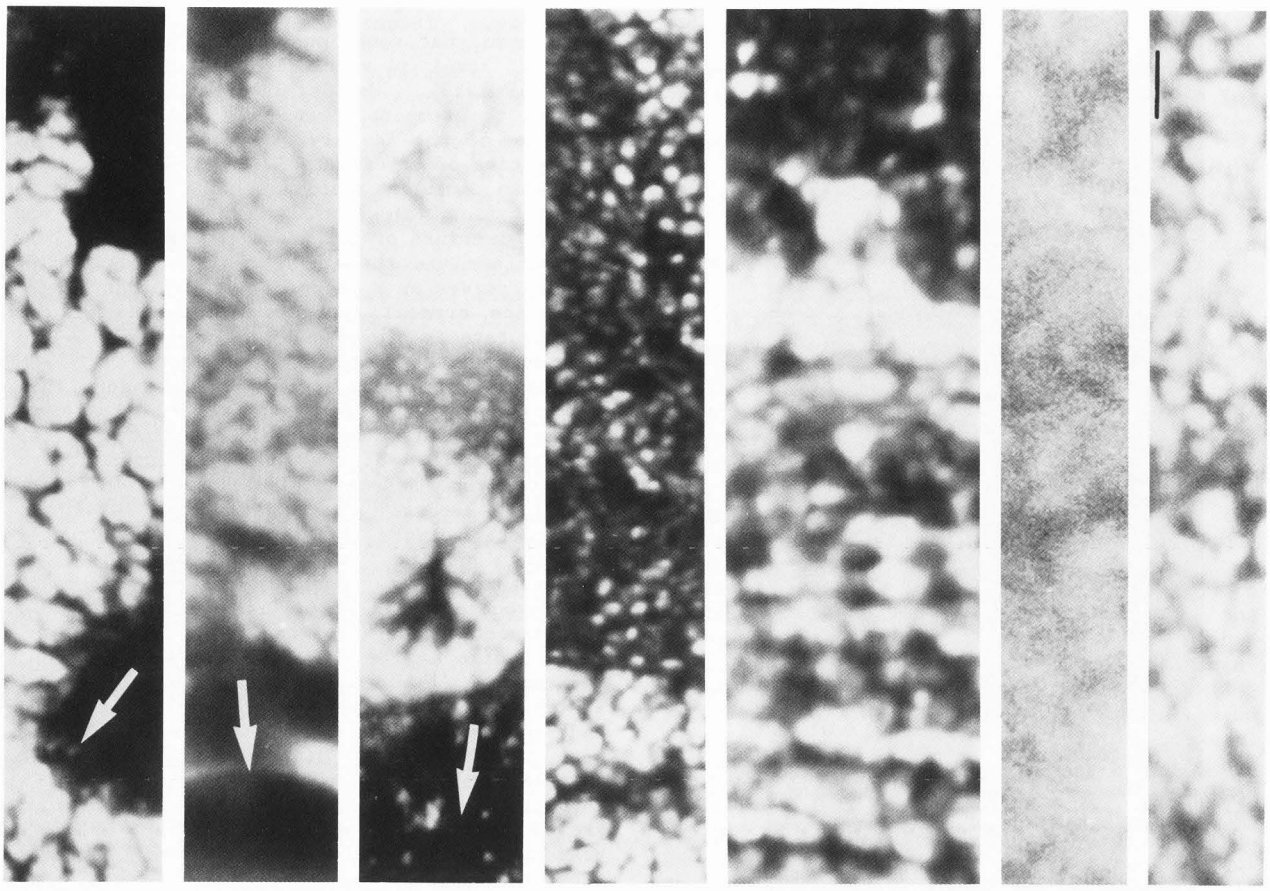

Fig. 4 Fig. 5 Fig. 6 Fig. 7 Fig. 8 Fig. 9 Fig. 10

Figs. 4-10. (Plate 1). Electron micrographs of 2 μm thick freeze-dried cryosections of various tissues which were quench cooled in liquid propane at -169°C. (This plate is from Cameron et al. 1985 and is republished here with the permission of Pacific Press, Inc., N.Y.). All of these micrographs were taken at a depth of at least 150 μm from the tissue/quenchant interface. The magnification factor is the same for all micrographs on this plate. Bar = 1.0 μm.

Fig. 4. Micrograph of the nucleus of a fully grown Xenopus oocyte. Notice the larger size of nuclear ice crystal imprints in the nucleoplasm compared to the open-cytoplasm (Figure 5) or the nucleolus (arrow).

Fig. 5. Micrograph of the cytoplasm of the same oocyte shown in fig. 4 showing a yolk platelet (arrow) with no ice crystal imprints.

Fig. 6. Shows a portion of a rat pancreatic acinar cell on the left. The arrow points to a zymogen granule with no ice crystal imprints. A portion of the nucleus with a nucleolus as well as the basal portion of the acinar cell are apparent.

Fig. 7. Shows portions of two rat hepatocytes. The larger ice crystal imprints on the top and bottom are within the nuclei while portions of the cytoplasm between the two nuclei show smaller ice crystal imprints.

Fig. 8. Shows relatively small ice crystal imprints within the erythrocytes on the top of the micrograph and relatively large ice crystal imprints within the cytoplasm of the rat cardiac myocyte on the bottom of the micrograph.

Fig. 9. Shows no recognizable ice crystal imprints in lens fibers of a rat.

Fig. 10. Shows ice crystal imprints in rat Achilles' tendon.

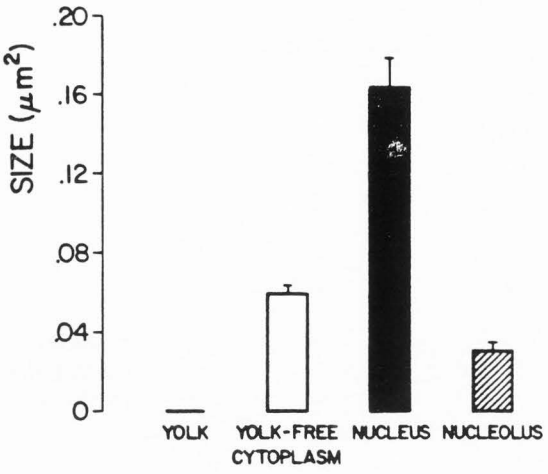

Fig. 11. Bar graph of the measured ice crystal imprint size (cross sectional area) differences among four subcellular compartments in the fully grown oocytes of the amphibian Xenopus. The mean size ± SEM of 20-80 ice crystal imprints is shown for each condition.

direct comparisons of ice crystal imprint size can be easily made.

The nucleus of the fully grown Xenopus oocyte, fig. 4, the pancreatic acinar cell (fig. 6) and the liver hepatocytes (fig. 7) all showed larger ice crystal imprints than areas of open cytoplasm in the same cell type. Several subcellular compartments within the cells illustrated in plate 1 show no evidence of ice crystal formation. These compartments included the yolk platelet in the oocyte cytoplasm (figure 5), the zymogen granules in the pancreatic acinar cell (fig. 6) and the open cytoplasm of the lens fiber cell (figure 9). The micrographs also show rather uniform ice crystal imprint size within a specific tissue compartment but show different sized ice crystal imprints among tissue types or among subcellular compartments. Figure 11 illustrates the quantitative differences in ice crystal imprint size among subcellular compartments in the case of the fully grown amphibian oocyte of Xenopus. The size of ice crystal imprints in erythrocytes (figure 8) was the same as the size of ice crystal imprints observed in erythrocytes from several other tissues (not illustrated). Thus the erythrocyte can serve as a useful reference for ice crystal imprint size in different tissues from the same animal. As illustrated in the region between the erythrocytes and the cardiac myocyte in figure 8, extracellular plasma always showed larger ice crystal imprints than within the tissue cells. It was also noted that cell membranes need not intervene between subcellular compartments with different size ice crystal imprints (i.e., the nucleolus and the nucleoplasm, fig. 4.

Correlations Between Ice Crystal Imprint Size and Water Content.

Quench cooled specimens of rather homogeneous composition were analyzed for ice crystal imprint size and water content to determine the relationship between the concentration and the nature of solutes and the growth of ice crystal imprints. A summary of our published observations on these relationships is shown in figure 12. The data reveal a general relationship between the radius ice crystal imprints of the specimens and water content. In general, those tissues with lower water content tend to have smaller sized ice crystal imprints. Notice however that those specimens enriched in parallel filamentous proteins have larger ice crystal imprints compared to the specimens enriched in globular proteins. This difference is attributed to enrichment in filamentous vs. globular protein composition as is dramatically illustrated by comparison of lens fiber (fig. 9) and the Achilles tendon (fig. 10) both of which happen to have the same water content. As shown in figure 12 those specimens enriched in filamentous proteins (tendon, skeletal muscle and cardiac muscle show a different linear relationship between water content (mass of solute per mass of water, Ms/M) and ice crystal imprint size than do those specimens enriched in globular proteins. The specimens enriched in globular proteins show a different linear regression line between the mass of solute per mass of water (Ms/M) values of 0.1 and 0.81.

To further explore the relationships between ice crystal imprint size and the concentration of globular proteins, we examined the influence of various concentrations of three different species of purified proteins (bovine serum albumin, hemoglobin, and lysozyme) on ice crystal imprint size under our quench cooling conditions. The results of these studies are illustrated in figures 13-15.

In the case of albumin an increase in its concentration caused a linear decrease in ice crystal imprint size until the point that ice crystal imprints were no longer visible (fig. 13). A linear regression analysis of the mean ice crystal imprint radius vs. the mass of solute per mass of water (Ms/M) gave an intercept on the Ms/M axis of 0.696. This intercept indicates that ice crystal imprints will reach undetectable dimensions at a concentration of about 144 g of water/100 g of dry protein powder. This suggests that at 144 g of water/100 g of protein mass, water was not able to diffuse to an ice crystal nucleation site during the quench cooling, thus no recognizable ice crystal imprints should be observed at this level of hydration.

A similar ice crystallization experiment was conducted for quench cooled samples of aqueous solutions of the globular protein, lysozyme. A linear regression analysis of the mean ice crystal imprint radius at Ms/M values of between 0.1 and 0.4 gave an intercept on the Ms/M axis of 0.787 equivalent to 127 g H_2O/100g

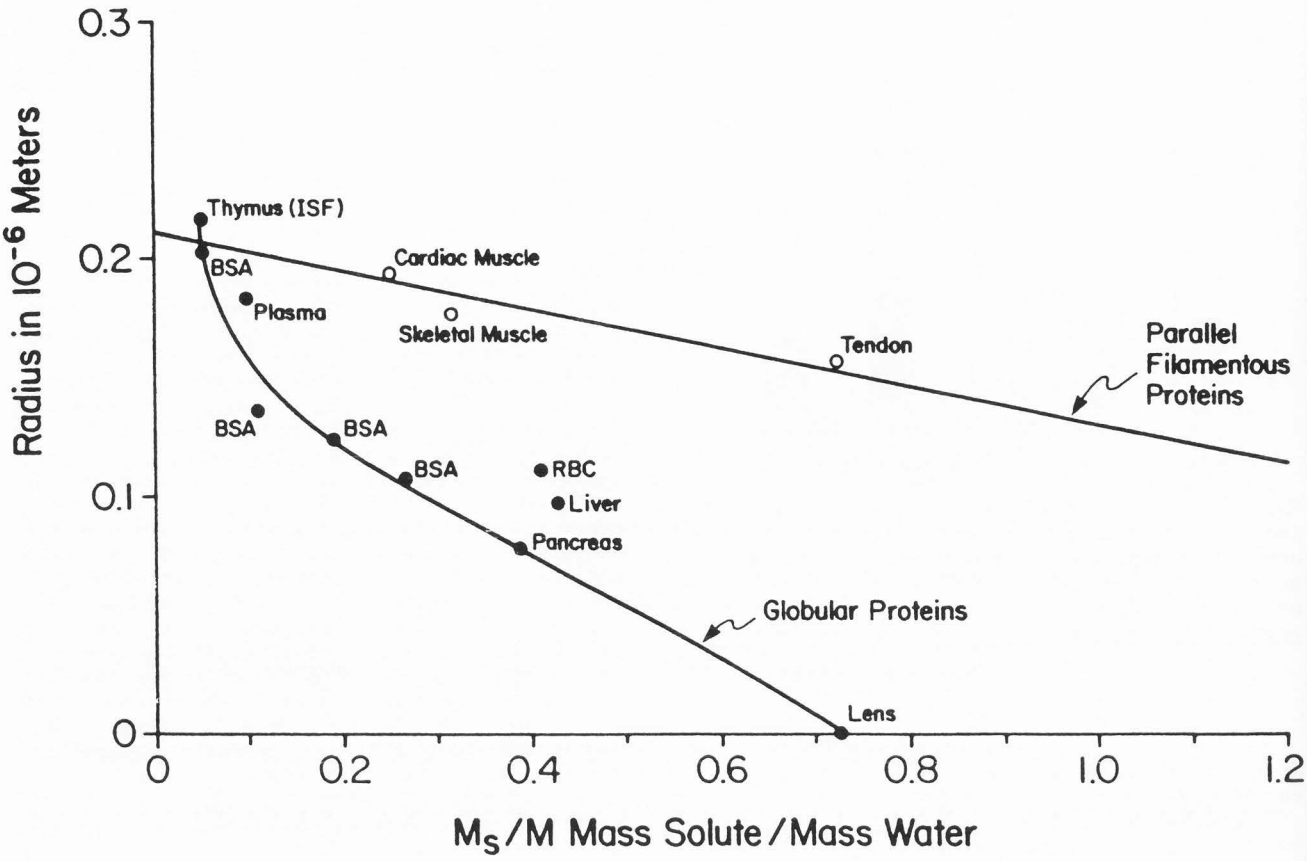

Fig. 12. Relationship between ice crystal imprint radius (r) and mass of solute per mass water (Ms/M). Tissues enriched in parallel filamentous proteins (cardiac muscle, skeletal muscle and tendon) were subjected to a linear regression analysis. The specimens enriched in globular proteins demark a significantly different linear regression line between Ms/M of 0.1 and 0.81. This figure is reproduced from Cameron et al., 1985 with permission of the original publishers (Pacific Press Inc., N.Y.).

lysozyme (fig. 14). At solute concentrations greater than Ms/M of 0.4 the size of ice crystal imprints no longer decreased in size but actually showed a significantly larger radius (fig. 14). Significant deviation from a linear relationship between ice crystal imprint radius and Ms/M at higher lysozyme concentration can be accounted for by the aggregation (polymerization or crystallization) of lysozyme molecules. For example upon making a lysozyme solution of 0.6g dry lysozyme per g water, protein crystals appeared in the vial within 12 h of powder dissolution.

Various concentrations of aqueous solutions of hemoglobin were quench-cooled and thin cryosections were cut and freeze-dried for ice crystal imprint size determinations. The results are presented in figure 15. A linear regression analysis of the mean ice crystal imprint size in the Ms/M range of 0.1 to < 0.3 gave an Ms/M axis intercept value of 0.696. This is equivalent to 144 g water/100 g dry hemoglobin. The next three higher concentrations of hemoglobin (fig. 15) showed significant ice crystal imprint size deviations from the linear relationship observed at the lower concentrations of hemoglobin. That these higher concentrations were associated with hemoglobin aggregation was confirmed by the frequent appearance of clusters of square edged hemoglobin crystals as seen in the STEM images of the cryosections from the two highest concentrations of hemoglobin. Thus there was direct evidence of increased hemoglobin aggregation into crystals at the highest concentrations of hemoglobin.

In general these observations show that the size ice crystal imprints decreases as the water content of the specimen decreases. However the pattern of decrease in ice crystal imprint size with increase in solute concentration seems to differ with or depend upon the composition of the macromolecular material in the specimen. Thus specimens enriched in globular proteins showed a more rapid rate of decrease in size of ice crystal imprints with increase in solute concentration than did specimens enriched in filamentous proteins. It also appeared that the aggregation of globular proteins was responsible for the growth of larger ice crystal imprints as described next.

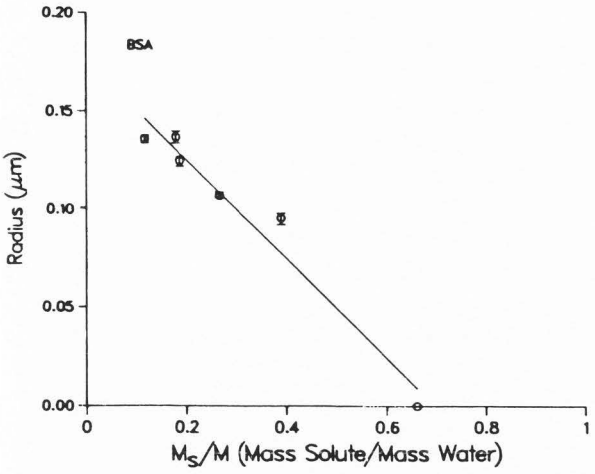

Fig. 13. Relationship between ice crystal imprint radius (in μm) and the mass of solute (dry bovine serum albumin) per mass water (Ms/M). The linear regression analysis fit of all six data points gave an intercept on the Ms/M axis of 0.696, equivalent to 144 g water per 100 g dry BSA. Notice that no ice crystals were observed at the highest BSA concentration.

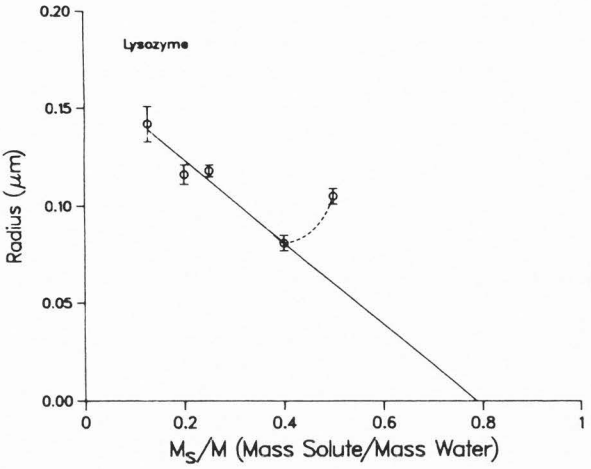

Fig. 14. Relationship between ice crystal imprint radius (in μm) and mass of dry lysozyme/mass water (Ms/M). The linear regression analysis fit of four data values on the left of the graph gave an intercept on the Ms/M axis of 0.787, equivalent to 127 g water/100 g dry lysozyme. The fifth point to the right (connected by a dashed line) showed a significant deviation from the linear relationship.

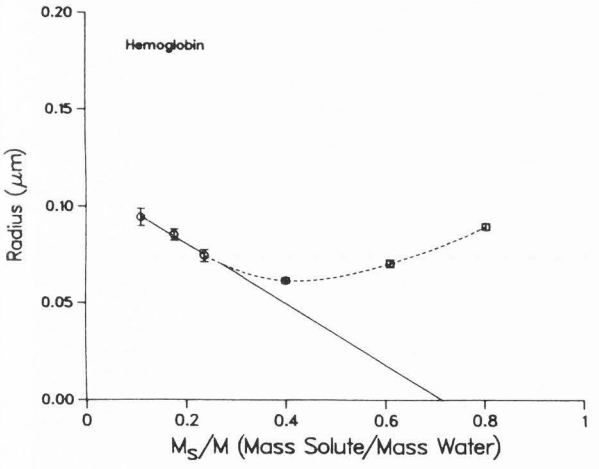

Fig. 15. Relationship between ice crystal imprint radius (in μm) and the mass of dry human hemoglobin A/mass water (Ms/M). The linear regression of the first three points on the left of the graph gave an intercept on the Ms/M axis of 0.696, equivalent to 144 g water per 100 g dry hemoglobin. The last three graph points to the right (connected by a dashed line) showed significant deviation from the linear relationship which was correlated with this visualization of protein crystals by STEM in the freeze-dried cryosections studied.

Influence of macromolecular aggregation on ice crystal imprint size.

As illustrated in figures 14-15, lysozyme and hemoglobin showed significant deviation from a linear decrease in ice crystal imprint size as the concentration of these globular proteins was increased above a specific Ms/M value. For lysozyme this value was above an Ms/M value of 0.4, while for hemoglobin it occurred below an Ms/M value of 0.4. In the case of bovine serum albumin (fig. 13) there was no evidence of deviation from a linear relationship between ice crystal imprint size and Ms/M. Indeed the highest concentration of BSA showed no evidence of ice crystal imprint growth indicating that diffusion of water molecules to ice crystal nucleation sites was not of sufficient magnitude to grow an ice crystal to a visible size.

Table 1 summarizes evidence that links aggregation of lysozyme and hemoglobin to the increase in ice crystal imprint size in the quench cooled specimens of lysozyme and hemoglobin at concentrations above Ms/M of 0.4. Table 1 also indicates that BSA did not aggregate into visible protein aggregates or crystals, even at an Ms/M value of > 0.6, which correlates with the fact that there was no significant deviations from linearity in the

Table 1. Summary of evidence that aggregation of proteins causes an increase in size of ice crystal imprints when a small sample (1-2 mm^3) was quench frozen in liquid propane cooled in liquid nitrogen.

Protein species	Evidence for or against aggregation change	Observed change in ice crystal imprint size in relation to aggregation
Lysozyme	Observed lysozyme crystal formation at higher concentrations[a]	Got larger at highest concentration[a]
	Observed a changed proton NMR-T_1 relaxation upon addition of 100 mM NaCl[b]	Got larger upon addition of 100 mM NaCl[c]
Bovine serum albumin (BSA)	No BSA crystals observed by electron microscopy of freeze-dried cryosections even at highest BSA concentration[a]	Continued to decrease at higher concentrations[a]
Human hemoglobin (Hb)	Hb crystallization observed by electron microscopy of freeze-dried cryosections[a]	Got larger at higher concentrations[a]
Actin	Addition of 5-200 mM KCl caused increased aggregation as shown by: formation of actin crystals (as seen by electron microscopy), increased viscosity (gelation)[d], larger sized particles as seen by analytical ultracentrifugation[e], significant changes in proton NMR-T_1 relaxation time[d].	Got larger upon addition of 200 mM KCl[d]
Tubulin brain extract with KCl, GTP and EGTA present[f]	Warming from 4°C to room temperature (24°C) caused: increased opacity and viscosity, and changed the proton NMR-T_1 relaxation time[g]	Prediction: Will get larger when warmed

[a] present study
[b] Addition of 100 mM NaCl to a 30 g dry lysozyme/100 g water solution shortened the T_1 relaxation time significantly (i.e. from 291±1 msec to 257±3 msec).
[c] Addition of 100 mM NaCl to a 25 g dry lysozyme/100 g water solution increased the ice crystal imprint radius significantly (i.e., from 0.10±.008 μm to 0.13±.005 μm)
[d] Cameron et al. (1987a)
[e] Fullerton et al. (1987)
[f] Fellous et al. (1977)
[g] Zimmerman et al. (1985)

size of ice crystal imprints at the higher concentrations. Together the evidence on these three globular proteins indicated that the aggregation of proteins was responsible for the observed increase in size of ice crystal imprints.

To assess the idea that the polymerization of actin molecules, (a major intracellular cytoskeletal protein), can influence ice crystal imprint size, we performed experiments with purified actin solutions (Cameron et al., 1987). Increasing amounts of KCl were added to a 12.4 mg/ml solution of purified actin and various observations and measures were made on the sample to determine the effect of this stepwise addition of KCl. The findings are presented in table 1 and in figure 16. The results indicate that the stepwise addition of KCl to the actin solution caused progressive actin polymerization, as judged by several reliable criteria. Samples of the actin solution were taken before addition of KCl and others were taken after addition of 200 mM KCl and were subjected to quench ice crystal imprint analysis. A significant increase in ice crystal imprint size in the sample of actin in 200 mM KCl was found (fig. 16). Thus the polymerization of a major cytoskeletal protein (actin) resulted in an increase in ice crystal imprint size and this suggested that a similar change in the polymerization of

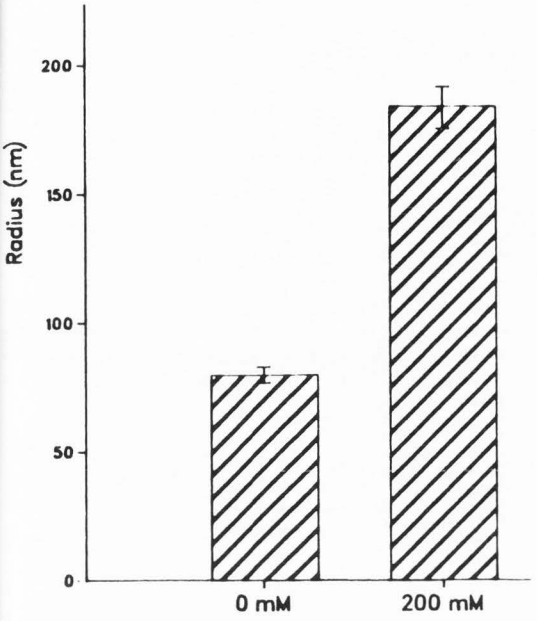

Fig. 16. Bar graph showing the effect of in vitro actin polymerization on ice crystal radius (μm). Actin polymerization was induced by raising the KCl concentration from 0 to 200 mM (see table 1 for a summary of evidence that polymerization of actin molecules did indeed occur due to this treatment). The mean and SE of 30 ice crystal imprints was measured in each actin sample. Actin polymerization resulted in significantly larger ice crystal imprints.

intracellular actin or other proteins would have a significant influence on ice crystal imprint size in cells.

We have, in fact, recently reported that significant changes in the size of cytoplasmic ice crystal imprints occurred during the first cell cycle of sea urchin eggs (Cameron et al., 1987). The changes were not due to water content change but were linked to polymerization and depolymerization of cytoplasmic actin (Cameron et al., 1987). These results have encouraged us to think that the quench ice crystal imprint size method is a useful method for study of interactions of macromolecules and water at a subcellular level.

Use of the Quench Ice Crystal Imprint Size Method for Determination of the Extent of Hydration Water on Globular Proteins in Aqueous Solution.

As shown in figures 13-15 an extrapolation of the linear portion of the ice crystal imprint size vs. solute concentration (Ms/M) curves for lysozyme, for bovine serum albumin and for hemoglobin to the Ms/M axis yields values of 0.787, 0.696 and 0.696, respectively. These Ms/M axis intercept values are interpreted to indicate that there is a constant quantity of water associated with globular protein species in aqueous solution and that this quantity of water was not incorporated into ice crystals during the quench cooling. The extrapolated Ms/M linear intercept value determines this quantity and suggests that this water fraction has a slowed rate of movement compared to bulk water.

Table 2. Comparison of the ice crystal imprint size method with other methods for determination of the extent of hydration water in g water/100g dry mass.

Protein species	Method	Amount	Reference
Lysozyme	Ice crystal imprint	127	This study
	x-ray diffraction	108-162[a]	Imoto et al. (1972)
	NMR titration	137	Fullerton et al. (1986)
	Liquid-gel transition	100	Finney et al. (1981)
Bovine serum albumin	Ice crystal imprint	144	This study
	NMR titration	145	Fullerton et al. (1987)
Human hemoglobin A	Ice crystal imprint	144	This study
	NMR titration	135	Cameron et al. (1988)
	Calculated from osmotic pressure	144	Cameron et al. (1988)

[a] estimated by authors from 2-3 layers over entire surface

Table 2 lists the extent of this motionally perturbed water for each of the three globular proteins studied by the quench ice crystal imprint method. Table 2 also lists the extent of hydration water associated with these proteins based on four other methods. There is good agreement between the five different methods used for determination of the extent of hydration water on these proteins. In conclusion, comparison of the ice crystal imprint size method for determination of the extent of hydration water and of the aggregated state of proteins in solution, yields data in agreement with macroscopic physicochemical methods. Thus the quench ice crystal imprint size method of analysis gives microscopic information about the interactions of macromolecules and water extending easily to the subcellular level of resolution.

References

Andrews SB, Mazurkiewicz JE, Kirk RG (1983). The distribution of intracellular ions in the avian salt gland. J. Cell Biol. 96, 1389-1399.

Bryan J, Kane RE (1982). Actin gelation in sea urchin egg extracts. Meth. in Cell Biol. 25, 176-199.

Cameron IL, Cook KR, Edwards D, Fullerton GD, Schatten G, Schatten H, Zimmerman AM, Zimmerman S (1987). Cell cycle changes in water properties in sea urchin eggs. J. Cell. Physiol. 133, 14-24..

Cameron IL, Ord VA, Fullerton GD (1988). Extent and properties of hydration water in human blood. Biochem. & Cell Biol. (in press).

Cameron IL, Hunter KE, Ord VA, Fullerton GD (1985). Relationships between ice crystal size, water content and proton NMR relaxation times in cells. Physiol. Chem. Phys. Med. NMR 17, 371-385.

Cameron IL, Hunter KE, Smith NKR (1983). Validation of quantitative energy-dispersive electron-probe X-ray microanalysis of electrolytes in thin cryosections of erythrocytes. In: Microbeam Analysis. Gooley R, (ed), San Francisco Press, San Francisco, CA. 237-242.

Elder H, Gray C, Jardine A, Chapman J, Biddlecombe W (1982). Optimum conditions for cryoquenching of small tissue blocks in liquid coolants. J. Microsc. 126, 45-62.

Fellous A, Francon J, Lennon AM, Nunez J (1977). Microtubule assembly in vitro purification of assembly-promoting factors. Eur. J. Biochem. 78, 167-174.

Finney JL, Goodfellow JM, Poole PL (1981). The structure and dynamics of water in globular proteins. In: Structural Molecular Biology, Davies DB, Saenger W, Danyluk SS, (eds), Plenum Press, NY, 387-426.

Franks F (1982). The properties of aqueous solutions at subzero temperatures. In: Water: A Comprehensive Treatise. 7, 215-338.

Frederick PM, Busing WM (1981). Ice crystal damage in frozen thin sections: freezing effects and their restoration. J. Microsc. 121, 191-199.

Fullerton GD, Cameron IL, Ord VA (1985). Orientation of tendon in the magnetic field and its effect on T_2 relaxation times. Radiology 155, 433-435.

Fullerton GD, Finnie MF, Hunter KE, Ord VA, Cameron IL (1987). The influence of macromolecular polymerization on spin-lattice relaxation of aqueous solutions. Mag. Reson. Imag. 5, (in press).

Fullerton GD, Ord VA, Cameron IL (1986). An evaluation of the hydration of lysozyme by an NMR titration method. Biochim. Biophys. Acta 869, 230-246.

Fullerton GD, Seitz PK, Hazlewood CF (1983). Application of the fast proton diffusion model to evaluation of water in artemia cysts. Physiol. Chem. Phys. Med. NMR 15, 489-499.

Hazlewood CF (1979). A view of the significance and understanding of the physical properties of cell-associated water. In: Cell Associated Water, Clegg J, Drost-Hanson W, (eds), Academic Press, NY, 165-259.

Heuser J (1981). Quick-freeze, deep-etch preparation of samples for 3-D electron microscopy. Trends Biochem. Sci. 6, 64-68.

Hirokawa N (1986). Quick-freeze, deep-etch of the cytoskeleton. Meth. in Enzymology 134, 598-612.

Imoto T, Johnson LN, North ACT, Phillips DC, Rupley JA (1972). In: The Enzymes, Boyer PD, (ed), Academic Press, NY, 7, 665-894.

Kuntz ID, Kauzmann W (1974). Hydration of proteins and polypeptides. Adv. in Protein Chem. 28, 239-349.

LaBadie D, Pool TB, Smith NKR, Cameron IL (1981). Elemental content in the nucleus in the yolk and yolk-free cytoplasm of developing Rana pipien oocytes: An X-ray microanalysis study. J. Cell. Physiol. 109, 91-97.

Lynch LJ (1983). Water relaxation in heterogeneous biological systems. In: Magnetic Resonance in Biology, Cohen JS, (ed), J. Wiley & Sons, Inc., NY, 248-304.

MacKenzie AP (1981). Modelling the ultra-

rapid freezing of cells and tissue. In: Microprobe Analysis of Biological Systems. Hutchinson TE, Somlyo AP (eds), Academic Press, NY, 397-421.

Merta PJ, Fullerton GD, Cameron IL (1986). Characterization of hydration water in unfertilized and fertilized sea urchin eggs. J. Cell. Physiol. 127, 439-447.

Rapatz GL, Menz LJ, Luyet BJ (1966). Anatomy of the freezing process in biological materials. In: Cryobiology. Meryman HT (ed), Academic Press, NY, 139-162.

Rebhun LI (1972). Freeze-substitution and freeze-drying. In: Principle and Techniques of Electron Microscopy. Biological Applications. Hayat MA (ed), Van Nostrand Reinhold, NY, 2, 3-49.

Schwabe KG, Terracio L (1980). Ultrastructural and thermocouple evaluation of rapid freezing techniques. Cryobiol. 17, 571-584.

Sonnenschein R, Heinzinger K (1983). A molecular dynamics study of water between Lennard-Jones walls. Chem. Phys. Letters 102, 550-554.

Spudick JA, Watts S. (1971). The regulation of rabbit skeletal muscle contraction. 1. Biochemical studies of the interaction of the tropomyosin-troponin complex with actin and proteolytic fragments of myosin. J. Biol. Chem. 246, 4866-4871.

Van Venrooij GEPM, Aertsen AMNJ, Hax WMA, Vewergaert PHJT, Verhoeven JJ (1975). Freeze etching. Freezing velocity and crystal size at different locations in samples. Cryobiol. 12, 46-61.

Zimmerman S, Zimmerman AM, Fullerton GD, Luduena RF, Cameron IL (1985). Water ordering during the cell cycle: nuclear magnetic resonance studies of the sea-urchin egg. J. Cell Sci. 79, 247-257.

Discussion with Reviewers

L. Edelmann: It is interesting that segregation compartment size analysis yields results on hydration water comparable to those of macroscopic physicochemical methods. I doubt however that the method is suited to answer the question how much cellular water is really influenced or perturbed by proteins or other macromolecules. It is conceivable that in areas which are not frozen very rapidly (10^5-10^6°C/s) proteins assume new configurations (before freezing) with the result that the interaction forces between these proteins and ions and water are completely changed. The validity of the described method should be tested with model systems and cells in which almost all water molecules are influenced by the macromolecules in such a way that they have reduced rotational diffusion coefficients compared to water molecules in dilute salt solutions (Trantham et al., Biophys. J. 45, 927-938, 1984; Rorschach (1985). In: Water and Ions in Biological Systems. Pullman A, Vasilescu V, Packer L, (eds), Plenum Press, NY, 729-736).

Authors: The quench ice crystal imprint size method has already been tested on two biological systems that have no bulk water as determined by NMR titration analysis (Fullerton GD, Cameron IL, in press, In: Principles and Applications of Biomedical MRI. Wehrle FW, Shaw D, Kneeland JB (eds), VCH Publisher, Inc., Deerfield FL, and Fullerton et al. (1985). One system is the lens fiber cells in situ and the other is fresh Achilles tendon. The results of quench cooling on ice crystal imprint size in these systems are illustrated in plate 1 of this paper. The lens and the tendon happen to have the same water content (1.4 g water/g dry mass) thus any difference in size of ice crystal imprints in the two tissues cannot be due to total water content. As expected from a specimen enriched in globular proteins with no bulk water, quench cooling of the lens cells resulted in no visible ice crystal imprints. The method therefore tested and confirmed that the lens cells contain no bulk water. On the other hand quench cooling of the tendon, which consists of parallel filamentous protein with no bulk water, showed ice crystal imprints. An explanation for this apparent paradox is presented in the text of the paper. These observations on tissues with no bulk water support the proposed quench cooling model. In the case of pure solutions of globular proteins, the quench ice crystal imprint method allows determination of the extent of hydration water and of the critical protein concentration (the concentration at which protein aggregation occurs). As you point out, the interpretation of results from cells and subcellular compartments is not as simple as in the case of pure solutions of globular proteins but can still provide insight into the extent of hydration water as illustrated by the lens results and changes in the degree of protein aggregation as shown by multiparameter studies over the first cell cycle of sea urchin eggs (Cameron et al., 1987).

H.E. Rorschach: The authors place great weight on the idea that diffusion of water molecules to the nucleation site plays a controlling role in determining the size of ice crystals. Is this so? Is diffusion important in the formation (growth) of ice crystals? In the first place, ice is less dense than water, so the molecules would have to move away from the growing crystal. In the second place, it seems to me that the rotational motion would be very important, since the orientation of the water molecule would have to fit the ice tetrahedral coordination. I would also suspect that the rate of propagation of the freezing temperature front compared with the orientation time (rotational and translational) of the water

molecules would be an important parameter.

Authors: Your statement that ice is less dense than water thus water molecules would have to move away from and not diffuse towards a growing ice crystal is true for pure water or for dilute solutions but does not hold for concentrated protein solutions such as occur in cells. For example, if one takes a unit volume of a 25 percent protein solution and converts the water in this unit volume to a single ice crystal, it would not occupy the entire original unit volume of the solution, even though freezing decreased the density of the water by a factor of 1.07. The reason is that the protein in the original unit volume of solution occupied a substantial volume fraction. The only way this single ice crystal can grow to larger size than the original unit volume of solution is for water molecules to diffuse to the crystal from outside the limits of the original unit volume of solution. Diffusion of water molecules to the ice crystal during cooling must therefore be an important factor in ice crystal growth in solutions of high protein concentration such as occur in cells.

Regarding your comment concerning the importance of rotational motion in the formation of ice. Because of the relatively rapid rotational correlation times of both bulk and structured water compartments ($> 10^{-11}$ S or faster), faster cooling rates than we used would be required before orientation of the water molecule to fit the ice tetrahedral coordination would become the limiting factor to ice crystal growth.

H.E. Rorschach: The authors suggest that diffusion measurements show that diffusion is more rapid parallel to the surfaces of filamentous proteins than it is perpendicular to the surfaces. I believe that the anisotropy can be entirely accounted for by the obstruction effects of the proteins, without any need for a microscopically anisotropic diffusion coefficient, as shown in Hazlewood (1979).

Authors: We agree that anisotropy of water diffusion exists along aligned filaments in muscle and do not challenge the idea that obstructions, due to proteins, are involved. However it also seems reasonable to assume that motions that carry the non-irrotationally bound water molecules along the surface of a filamentous protein towards an ice crystal might be more rapid than those away from the surface at a microscopic level. Such a suggestion is supported by the simulation studies of water on and near hard walls (Sonnenschein and Heinzinger, 1983).